Available online at www.sciencedirect.com
SCIENCE DIRECT
Journal of Sound and Vibration 296 (2006) 714–733
JOURNAL OF SOUND AND VIBRATION
www.elsevier.com/locate/jsvi

Critical excitation of sdof elasto-plastic systems

S.K. Au*

Department of Building and Construction, City University of Hong Kong, 83 Tat Chee Avenue, Kowloon, Hong Kong

Received 25 October 2005; received in revised form 5 January 2006; accepted 24 January 2006
Available online 10 July 2006

Abstract

The critical excitation of a dynamical system is defined as the input excitation with the lowest energy that drives the system from one specified state to another within a given time span. Critical excitations play an important role in first passage problems because they are the most probable point in the first passage failure region of the standard Normal stochastic load space. They may also be used to provide efficient solution of other stochastic analysis problems by means of asymptotic approximations. Although the solution of critical excitation for linear systems can be obtained through unit impulse response functions, the case of nonlinear hysteretic systems is still under research. The latter has important relevance in the study of nonlinear response of structures under severe earthquake loads, where the characteristics of critical excitations may aid understanding the collapse potential of earthquakes. This paper investigates the critical excitation of single-degree-of-freedom (sdof) elasto-plastic systems. Through observations on dynamic characteristics, the critical excitation is parameterized in the time domain that allows for its efficient numerical solution. It is found that, in addition to resonance phenomenon that is observed in linear systems, a mechanism called 'boundary criticality' is responsible for driving elasto-plastic systems to its target by maximizing the capability of gaining momentum during elastic loading while avoiding opposing plastic deformations.

1. Introduction

Let $y(t)$ denote the displacement response of an elasto-plastic system, satisfying the governing equation

$$\ddot{y}(t) + 2\zeta\omega\dot{y}(t) + F_r(y) = f(t), \tag{1}$$

where ζ is the elastic critical damping ratio, ω is the elastic circular frequency (in rad/s), f is the excitation and $F_r(y)$ is the restoring force. The restoring force is given by $\omega^2 y(t)$ before first yielding at $y = +/-b_0$. In the context of this study, the problem of critical excitation is to find the excitation with minimum 'energy' (to be defined shortly) that drives the response y of the single-degree-of-freedom (sdof) elasto-plastic system from rest (i.e., $y(0) = 0$, $\dot{y}(0) = 0$) to the threshold level b_f at a specified time instant t_f. The 'energy' E of an

*Tel.: +852 2194 2769; fax: +852 2788 7612.
E-mail address: siukuiau@cityu.edu.hk.

0022-460X/$ - see front matter © 2006 Elsevier Ltd. All rights reserved.
doi:10.1016/j.jsv.2006.01.034

excitation is defined through its L_2-norm,

$$E(f) = \frac{1}{2}\int_0^\infty f(\tau)^2 \, d\tau. \tag{2}$$

Utilizing critical excitations for solving dynamic problems was independently advocated by Papoulis [1] and Drenick [2]. Critical excitations are relevant in both deterministic and stochastic problems of vibrations. In the deterministic context, they are related to the control law with minimum energy that drives a system from one state to another [3]. In a stochastic context, they are the most probable excitation in the first passage failure region of the standard Normal load space for systems subjected to white noise excitations. They provide bounds for maximum response under constraints in the input energy. They have also been used as 'design points' for constructing importance sampling densities for efficient estimation of first passage failure probabilities (e.g., [4,5]). Elasto-plastic sdof systems, despite their sdof nature, have been frequently studied for gaining insights into multi-degree-of-freedom (mdof) systems [6–11].

The critical excitation problem can be posed as a constrained optimization problem using Lagrange multipliers, where the objective function $J(f, \lambda)$ is minimized with respect to f and λ:

$$J(f, \lambda) = \frac{1}{2}\int_0^{t_f} f^2 \, d\tau + \lambda[b_f - y(t_f)] \tag{3}$$

with y governed by Eq. (1). Note that the elasto-plastic system is causal, i.e., future excitation does not affect the response in the past or at present. It then follows that the critical excitation will be identically zero for $t > t_f$, since any nonzero excitation after t_f cannot change the response on $[0, t_f]$ but will always imply higher energy in the excitation and hence a suboptimal configuration. It is therefore sufficient to consider optimization over the class of excitations for which $f(t) \equiv 0$ for $t > t_f$. Effectively, this consideration has reduced the upper limit of the integral in Eq. (3) from ∞ to t_f.

When the system is linear-elastic, i.e., $F_r(y) \equiv \omega^2 y$ for all y, the critical excitation can be obtained readily using Calculus of Variation [1,2]. Other studies have been devoted to the linear problem under the context of random vibrations with constraints in the power spectral density function and with nonstationary characteristics [12–14].

Critical excitations for nonlinear hysteretic systems are much more difficult to obtain than for linear systems. Most studies focused on sdof systems, but even in this case exact solutions have not been obtained. When the system in Eq. (1) is elasto-plastic, Calculus of Variation cannot be applied directly because the first variation of y with respect to f is difficult to obtain in close form. Iyengar [15] studied elastic nonlinear systems and provided bounds for their maximum response under deterministic and stochastic inputs. Westermo [16] considered maximizing the input energy density (i.e., work done by excitation per cycle) within the class of excitations spanned by the displacement (y) and velocity ($\dot{y}$) response. Approximate periodic solutions were obtained numerically for the critical response of sdof elasto-plastic systems. The relationship between resonance frequency and response amplitude was numerically obtained, which exhibited complex behavior such as multiple critical harmonics not observed in linear systems. Equivalence linearization [17,18] has also been used for approximate solution in the frequency domain [19–21]. Koo and co-workers [22] recently showed that for nonlinear elastic systems at sufficiently large first passage time the critical excitation is identical to one that generates the mirror image of the free-vibration response when the system is released from the target level. They also applied the result as an approximation for nonlinear-hysteretic systems. It should be noted that this result also holds for linear-elastic systems and is a consequence of the elastic nature of the restoring force, in that the behavior is the same regardless of progressing forward or backward in time.

In this work, we obtain the critical excitation of sdof elasto-plastic systems by solving the constrained optimization problem where the excitation is parameterized in the time domain. The paper is organized as follows. We first present in Section 2 a general time-domain parametric form of excitations that are candidates for being a critical excitation. The parameterization scheme considers the time history of excitation as a sequence of segments according to the time instants at which the response transits between different characteristic phases (e.g., elastic loading/unloading, plastic loading). The critical excitation problem then corresponds to optimizing with respect to the number of segments, the discrete parameters (referred as 'boundary state parameters') defining the different segments as well as the excitation time history within each segment. By construction, a single governing equation follows within each segment, and so the optimization of

the corresponding excitation time history can be solved analytically by Calculus of Variation, the details of which will be presented in Section 3. The remaining optimization with respect to the boundary state parameters will be discussed in Section 4, where physical arguments are used to reduce the number of parameters. For this purpose, we introduce one crucial phenomenon called 'boundary criticality', which describes the tendency of the critical response to touch the elastic/plastic boundary in order to maximize its velocity to produce large plastic excursions. The recognition of boundary criticality allows further reduction of the number of boundary state parameters, leading to an efficient numerical scheme for finding the critical excitation. This will be presented in Section 5. Finally, a numerical study is presented in Section 6 for investigating the nature of critical excitations.

2. Parametric form of critical excitation

Consider the response y due to some excitation f that is a candidate for critical excitation, as shown in Fig. 1. The figure has incorporated a number of features about the critical excitation that will be discussed next.

The response starts linear-elastically from rest (O) and reaches its yield displacement b_0 at τ_1 (A), after which it makes an excursion into the plastic regime, achieving a local maximum (B), and then returns to the linear-elastic regime again as it decreases with unloading of the restoring force. Subsequently, the response enters the plastic regime again to make another excursion, and this cycle may repeat until the final threshold level is reached. For $b_f > b_0$, the first passage point at b_f must occur in the plastic regime, since otherwise it must have undergone elastic unloading from a displacement that is greater than b_f, which implies that the first passage point occurs earlier, leading to a contradiction.

The final phase involves reaching the level b_f where it achieves a local maximum at F. Strictly speaking, the velocity at F is not necessarily zero, since it is not specifically constrained in the problem. However, unless the failure time is very small compared to the natural period, the amount of overshoot is often insignificant. A mathematical proof of this statement is provided in Ref. [23]. It is often a good approximation to assume that the final state has zero velocity.

We have ruled out the possibility that the critical response may excur downward below $-b_0$ into the plastic regime (here referred as having a 'negative plastic deformation'), as it is argued in Appendix A that for every response that has a negative plastic deformation it is always possible to construct another response without negative plastic deformation that has a smaller energy, making the former always sub-optimal and thus can be ruled out when the critical excitation is sought.

The response is configured such that the displacement and velocity at the transition points between the elastic and plastic regime are explicitly parameterized. The advantage of this is that within each segment only one governing equation applies and hence linear-elastic and plastic phases can be handled separately. The segments spanned by τ_i, $i = 1, \ldots, n$ are all linear-elastic. The segments spanned by γ_i, $i = 1, \ldots, n$, are plastic, during which $y(t)$ is non-decreasing. For given $\tau_i, \gamma_i, v_i, b_i$, $i = 1, \ldots, n$, each segment can be optimized independently of each other using the Calculus of Variation, since the optimal solution within each segment only depends on their boundary states (displacement and velocity). This idea in principle reduces the original nontrivial Calculus of Variation problem into a sequence of standard ones that can be solved readily, which

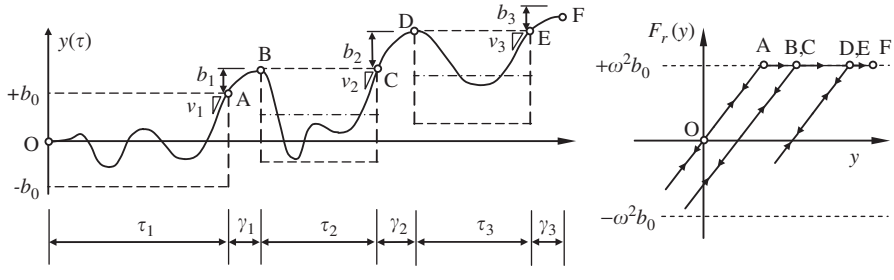

Fig. 1. Schematic diagram for critical response.

will be presented in the next section. Of course, the parameters $\tau_i, \gamma_i, v_i, b_i$, $i = 1, \ldots, n$ as well as the number of segments n should be subsequently optimized to yield the critical excitation.

3. Critical excitation for given boundary states

The critical excitation time history within each parameterized segment (linear-elastic or plastic phase) with given boundary states is derived in this section. The results will be applied frequently in later sections.

3.1. Linear-elastic phase

The critical excitation that drives the system from the state (y_i, v_i) to (y_f, v_f) in time t_f on the $(y, \dot{y})$ state-space is derived here. The response y that starts with $y(0) = y_i$, $\dot{y}(0) = v_i$ and subjected to excitation f can be generally expressed as

$$y(t) = y_i\, g(t) + v_i\, h(t) + \int_0^t h(t-\tau) f(\tau)\, \mathrm{d}\tau, \tag{4}$$

where

$$h(t) = \frac{\mathrm{e}^{-\zeta\omega t}}{w_d} \sin \omega_d t \tag{5}$$

is the unit impulse response, being identical to the free vibration response with zero initial displacement and unit initial velocity; and

$$g(t) = \mathrm{e}^{-\zeta\omega t}\left(\cos \omega_d t + \frac{\zeta}{\sqrt{1-\zeta^2}} \sin \omega_d t\right) \tag{6}$$

is the free vibration response with unit initial displacement and zero initial velocity. Differentiating Eq. (4) with respect to t, the velocity response is given by

$$\dot{y}(t) = y_i\, \dot{g}(t) + v_i\, \dot{h}(t) + \int_0^t \dot{h}(t-\tau) f(\tau)\, \mathrm{d}\tau. \tag{7}$$

To reach the final state (y_f, v_f) with minimum energy, the following objective function should be minimized:

$$J(f, \beta_1, \beta_2) = \frac{1}{2}\int_0^{t_f} f^2\, \mathrm{d}\tau + \beta_1[y_f - y(t_f)] + \beta_2[v_f - \dot{y}(t_f)], \tag{8}$$

where β_1 and β_2 are Lagrange multipliers, $y(t_f)$ and $\dot{y}(t_f)$ are obtained from Eqs. (4) and (7), respectively. The first variation of J with respect to f is

$$\delta J = \int_0^{t_f} f\, \delta f\, \mathrm{d}\tau - \beta_1 \delta y(t_f) - \beta_2 \delta \dot{y}(t_f), \tag{9}$$

where $\delta y(t_f) = \int_0^{t_f} h(t-\tau)\delta f\, \mathrm{d}\tau$ and $\delta \dot{y} = \int_0^{t_f} \dot{h}(t-\tau)\delta f\, \mathrm{d}\tau$. Substituting $\delta y(t_f)$ and $\delta \dot{y}(t_f)$ into Eq. (9) and requiring $\delta J = 0$ to hold for all arbitrary δf yields the critical excitation

$$f^*(\tau) = \beta_1 h(t_f - \tau) + \beta_2 \dot{h}(t_f - \tau). \tag{10}$$

Substituting Eq. (10) into Eqs. (4) and (7), and enforcing the final conditions $y(t_f) = b_f$ and $\dot{y}(t_f) = v_f$, yields the following linear matrix equation for $\underline{\beta} = [\beta_1, \beta_2]^{\mathrm{T}}$:

$$\underline{H}(t_f)\, \underline{\beta} = \underline{L}_1(t_f)\, \underline{x}, \tag{11}$$

where $\underline{x} = [y_i, v_i, y_f, v_f]^{\mathrm{T}}$ is a vector of the boundary state values, and

$$\underline{H}(t_f) = \begin{bmatrix} h_{11}(t_f) & h_{12}(t_f) \\ h_{12}(t_f) & h_{22}(t_f) \end{bmatrix}, \tag{12}$$

$$h_{11}(t_f) = \int_0^{t_f} h^2 \,\mathrm{d}\tau, \quad h_{12}(t_f) = \int_0^{t_f} h\dot{h} \,\mathrm{d}\tau = h(t_f)^2/2, \quad h_{22}(t_f) = \int_0^{t_f} \dot{h}^2 \,\mathrm{d}\tau, \tag{13}$$

$$\underline{L}_1(t_f) = \begin{bmatrix} -g(t_f) & -h(t_f) & 1 & 0 \\ -\dot{g}(t_f) & -\dot{h}(t_f) & 0 & 1 \end{bmatrix}. \tag{14}$$

Noted that $\underline{H}$ is a symmetric matrix with positive entries.

Writing $f = [h(t_f - \tau), \dot{h}(t_f - \tau)]\ \underline{\beta}$ and using Eq. (11), the energy of the critical excitation can be obtained as

$$E(f^*) = \frac{1}{2}\int_0^{t_f} f^{*2} \,\mathrm{d}\tau = \frac{1}{2}\,\underline{\beta}^{\mathrm{T}}\,\underline{H}\,\underline{\beta} = \frac{1}{2}\,\underline{x}^{\mathrm{T}}\underline{L}_1^{\mathrm{T}}\underline{H}^{-1}\underline{L}_1\,\underline{x} \tag{15}$$

which is a quadratic form of the boundary state vector $\underline{x}$.

3.2. Plastic phase

We next consider the critical excitation that drives the response in the plastic regime from (b_0, v) to $(b_0 + b_1, 0)$ on the $(y, \dot{y})$ state-space in time s. The governing equation in this case is given by

$$\ddot{y}(t) + 2\zeta\omega\dot{y}(t) + \omega^2 b_0 = f(t) \tag{16}$$

with the initial conditions $y(0) = b_0$ and $\dot{y}(0) = v$. Let $z(t) = y(t) - b_0$, then $z(t)$ has the initial conditions $z(0) = 0$, $\dot{z}(0) = v$ and satisfies

$$\ddot{z}(t) + 2\zeta\omega\dot{z}(t) = F(t), \tag{17}$$

where $F(t) = f(t) - \omega^2 b_0$. The response for z with a unit impulse in F is given by

$$r(t) = \frac{1}{2\zeta\omega}(1 - \mathrm{e}^{-2\zeta\omega t}). \tag{18}$$

The solution for z subjected to f can thus be obtained as

$$\begin{aligned} z(t) &= vr(t) + \int_0^t r(t-\tau)F(\tau)\,\mathrm{d}\tau \\ &= vr(t) + \int_0^t r(t-\tau)f(\tau)\,\mathrm{d}\tau - \omega^2 b_0 \int_0^t r(\tau)\,\mathrm{d}\tau. \end{aligned} \tag{19}$$

Note that the constraints $y(s) = b_0 + b_1$ and $\dot{y}(s) = 0$ are equivalent to $z(s) = b_1$ and $\dot{z}(s) = 0$, and so the objective function to be minimized is

$$J(f, \chi_1, \chi_2) = \frac{1}{2}\int_0^s f^2 \,\mathrm{d}\tau + \chi_1[b_1 - z(s)] + \chi_2[-\dot{z}(s)], \tag{20}$$

where χ_1 and χ_2 are Lagrange multipliers. Applying Calculus of Variation yields the critical excitation as

$$f(\tau) = \chi_1 r(s-\tau) + \chi_2 \dot{r}(s-\tau), \tag{21}$$

where $\underline{\chi} = [\chi_1, \chi_2]^{\mathrm{T}}$ is found from the following matrix equation:

$$\underline{R}(s)\ \underline{\chi} = \underline{L}(s)\ \underline{x} \tag{22}$$

with $\underline{x} = [b_0, v, b_1]^{\mathrm{T}}$,

$$\underline{R}(s) = \begin{bmatrix} r_{11}(s) & r_{12}(s) \\ r_{12}(s) & r_{22}(s) \end{bmatrix}, \tag{23}$$

$$r_{11}(s) = \int_0^s r^2 \,\mathrm{d}\tau, \quad r_{12}(s) = \int_0^s r\dot{r} \,\mathrm{d}\tau = r(s)^2/2, \quad r_{22}(s) = \int_0^s \dot{r}^2 \,\mathrm{d}\tau \tag{24}$$

and

$$\underline{L}_2(s) = \begin{bmatrix} \omega^2 \int_0^s r\,\mathrm{d}\tau & -r(s) & 1 \\ \omega^2 r(s) & -\dot{r}(s) & 0 \end{bmatrix}. \tag{25}$$

Note that $\int_0^s r\,\mathrm{d}\tau$ and $\dot{r}(s)$ can be obtained analytically. The energy corresponding to the critical excitation in this case is given by

$$E(f^*) = \tfrac{1}{2}\underline{\chi}^{\mathrm{T}}\,\underline{R}\,\underline{\chi} = \tfrac{1}{2}\underline{x}^{\mathrm{T}}\underline{L}_2^{\mathrm{T}}\underline{R}^{-1}\underline{L}_2\,\underline{x}. \tag{26}$$

The results here take the same form as those in the linear case, which is not surprising because the governing equation (Eq. (17)) is still linear.

4. Optimization of boundary state parameters

The last section obtains analytical solution for the segment of critical excitation given that the boundary state parameters, i.e., the length of the segment and its boundary states (displacement and velocity), are specified. The boundary state parameters should be further optimized in order to yield the critical excitation, which is considered in this section. It will be seen that the objective function to be minimized can be reduced by recognizing some qualitative feature of the problem.

Using results from the last section, the critical excitation for the different segments can be obtained for given values of $\tau_i, \gamma_i, b_i, v_i$; $i = 1, \ldots, n$. The resulting energy of the 'partially' optimized excitation can be written as

$$E_n(\underline{\theta}) = \sum_{i=1}^{n} A_i(\tau_i, \gamma_i, v_i, b_i), \tag{27}$$

where $\underline{\theta} = [\tau_i, \gamma_i, b_i, v_i : i = 1, \ldots, n]^{\mathrm{T}}$ collects the set of parameters and $A_i(\tau_i, \gamma_i, v_i, b_i)$ is the energy of the ith segment of the critical excitation. For $i = 1$, $A_1(\tau_1, \gamma_1, v_1, b_1)$ is given by the sum of Eq. (15) with $\underline{x} = [0, 0, b_0, v_1]^{\mathrm{T}}$ and Eq. (26) with $\underline{x} = [b_0, v_1, b_1]^{\mathrm{T}}$. For the subsequent segments, $A_i(\cdot,\cdot,\cdot,\cdot)$, $i = 2, \ldots, n$, are identical because they correspond to the same problem, namely, going with minimum energy linear-elastically on the $(y, \dot{y})$ state-space from $(b_0, 0)$ to (b_0, v_i) and then plastically from (b_0, v_i) to $(b_0 + b_1, 0)$. Thus, letting $A_i = A_2$ for all $i = 2, \ldots, n$, Eq. (27) can be re-written as

$$E_n(\underline{\theta}) = A_1(\tau_1, \gamma_1, v_1, b_1) + \sum_{i=2}^{n} A_2(\tau_i, \gamma_i, v_i, b_i). \tag{28}$$

To obtain the critical excitation for a given n, we need to minimize $E_n(\underline{\theta})$ with respect to $\underline{\theta}$ subject to the constraints $\sum_{i=1}^{n} \tau_i + \gamma_i = t_f$ and $\sum_{i=1}^{n} b_i = b_f - b_0$, and the constraint that within each segment the response must remain within the assumed regime (linear-elastic or plastic). The last requirement is to ensure that the expressions used for A_i are valid. The objective function to be optimized is given by

$$\begin{aligned} J_n(\underline{\theta}, \lambda_1, \lambda_2) = {} & A_1(\tau_1, \gamma_1, v_1, b_1) + \sum_{i=2}^{n} A_2(\tau_i, \gamma_i, v_i, b_i) \\ & + \lambda_1 \left(t_f - \sum_{i=1}^{n} \tau_i + \gamma_i \right) + \lambda_2 \left(b_p - \sum_{i=1}^{n} b_i \right), \end{aligned} \tag{29}$$

where λ_1 and λ_2 are Lagrange multipliers. The last constraint is not explicitly reflected in the objective function but may be in principle enforced by checking the resulting solution.

For a given n, there are $(4n + 2)$ parameters to be optimized. To simplify the optimization problem, it is noted that for given λ_1 and λ_2, the optimality equations for the parameters $\tau_i, \gamma_i, v_i, b_i$ of different segments are uncoupled, i.e., $\tau_i, \gamma_i, v_i, b_i$ can be solved without knowing the optimal values of $\tau_j, \gamma_j, v_j, b_j$, $j \neq i$. In addition, the optimization problem can be simplified substantially by exploiting some physical features of the critical excitation problem, which are presented in the following sub-sections.

4.1. Symmetry

For $i = 2, \ldots, n$, the parameters $\tau_i, \gamma_i, v_i, b_i$ appear in the objective function in Eq. (29) through the same function A_2. Consequently, they are symmetric, in the sense that the value of J is unaltered when the set of values $\{\tau_i, \gamma_i, v_i, b_i\}$ and $\{\tau_j, \gamma_j, v_j, b_j\}$ $(i \neq j)$ are swapped. Assuming a global optimum exists for the critical excitation and hence for the set of parameters $\underline{\theta}$, this means that the critical excitation will have $\tau_2 = \tau_3 = \cdots = \tau_n$; $\gamma_2 = \gamma_3 = \cdots = \gamma_n$; $v_2 = v_3 = \cdots = v_n$; $b_2 = b_3 = \cdots = b_n$. This observation reduces the dimension of the optimization problem from $(4n + 2)$ to $4 + 4 + 2 = 10$, where the set of parameters to be optimized is reduced to $\underline{\theta} = [\tau_1, \gamma_1, v_1, b_1, \tau_2, \gamma_2, v_2, b_2]^{\mathrm{T}}$, λ_1, and λ_2. With this consideration, it suffices to consider the objective function

$$\begin{aligned} J_n(\underline{\theta}, \lambda_1, \lambda_2) = {} & A_1(\tau_1, \gamma_1, v_1, b_1) + (n-1)A_2(\tau_2, \gamma_2, v_2, b_2) \\ & + \lambda_1[t_f - (\tau_1 + \gamma_1) - (n-1)(\tau_2 + \gamma_2)] \\ & + \lambda_2[b_f - b_0 - b_1 - (n-1)b_2]. \end{aligned} \tag{30}$$

Correspondingly, the candidate critical response is now reduced to one with identical segments starting from the second segment and onwards.

4.2. Analytical solution for optimal velocity

The optimal value of v_i can be obtained analytically in terms of other parameters, because the objective function is quadratic in v_i. From Eq. (30), $\partial J_n/\partial v_1 = 0$ gives $\partial A_1/\partial v_1 = 0$, where

$$A_1(\tau_1, \gamma_1, v_1, b_1) = \frac{1}{2}\begin{bmatrix} 0 \\ 0 \\ b_0 \\ v_1 \end{bmatrix}^{\mathrm{T}} \underline{L}_1(\tau_1)^{\mathrm{T}}\, \underline{H}(\tau_1)^{-1}\, \underline{L}_1(\tau_1) \begin{bmatrix} 0 \\ 0 \\ b_0 \\ v_1 \end{bmatrix} + \frac{1}{2}\begin{bmatrix} b_0 \\ v_1 \\ b_1 \end{bmatrix}^{\mathrm{T}} \underline{L}_2(\gamma_1)^{\mathrm{T}}\, \underline{R}^{-1}(\gamma_1)\, \underline{L}_2(\gamma_1) \begin{bmatrix} b_0 \\ v_1 \\ b_1 \end{bmatrix} \tag{31}$$

and $\underline{H}$, $\underline{L}_1$, $\underline{R}$ and $\underline{L}_2$ are given by Eqs. (12), (14), (23) and (25), respectively. Differentiating Eq. (31) with respect to v_1 gives a linear expression in v_1:

$$\frac{\partial A_1}{\partial v_1} = \begin{bmatrix} 0 \\ 0 \\ 0 \\ 1 \end{bmatrix}^{\mathrm{T}} \underline{L}_1(\tau_1)^{\mathrm{T}}\, \underline{H}(\tau_1)^{-1}\, \underline{L}_1(\tau_1) \begin{bmatrix} 0 \\ 0 \\ b_0 \\ v_1 \end{bmatrix} + \begin{bmatrix} 0 \\ 1 \\ 0 \end{bmatrix}^{\mathrm{T}} \underline{L}_2(\gamma_1)^{\mathrm{T}}\, \underline{R}^{-1}(\gamma_1)\, \underline{L}_2(\gamma_1) \begin{bmatrix} b_0 \\ v_1 \\ b_1 \end{bmatrix} \tag{32}$$

from which the optimal value of v_1, denoted by $\hat{v}$, can be obtained in terms of τ_1, γ_1 and b_1:

$$\hat{v}_1(\tau_1, \gamma_1, b_1) = -\frac{P_{43}(\tau_1) + Q_{21}(\gamma_1)}{P_{44}(\tau_1) + Q_{22}(\gamma_1)} b_0 - \frac{Q_{23}(\gamma_1)}{P_{44}(\tau_1) + Q_{22}(\gamma_1)} b_1, \tag{33}$$

where $P = \underline{L}_1^{\mathrm{T}} \underline{H}^{-1} \underline{L}_1$, $Q = \underline{L}_2^{\mathrm{T}} \underline{R}^{-1} \underline{L}_2$, and P_{ij} denotes the (i,j)-entry of P. Expressions for P_{ij} and Q_{ij} are provided in Appendix B. Using a similar procedure, $\hat{v}_2$ can be obtained in terms of τ_2, γ_2 and b_2:

$$\hat{v}_2(\tau_2, \gamma_2, b_2) = \frac{P_{41}(\tau_2) - P_{43}(\tau_2) - Q_{21}(\gamma_2)}{P_{44}(\tau_2) + Q_{22}(\gamma_2)} b_0 - \frac{Q_{23}(\gamma_2)}{P_{44}(\tau_2) + Q_{22}(\gamma_2)} b_2. \tag{34}$$

The optimal solution for v_1 and v_2 can be substituted into the objective function Eq. (30) for further optimization, where the set of parameters to be optimized is reduced to $\underline{\theta} = [\tau_1, \gamma_1, b_1, \tau_2, \gamma_2, b_2]$, λ_1 and λ_2 (total 8 parameters).

The optimality condition $\partial A_1/\partial v_1 = 0$ for v_1 in Eq. (32) bears an interesting but nontrivial interpretation. Appendix C shows that it is equivalent to continuity of the excitation at the moment where the response transits from the elastic to plastic regime. A counterpart result holds for the optimality condition regarding v_2.

4.3. Boundary criticality

We next argue that, under the usual case of interest where t_f is not too small compared to the elastic natural period $T = 2\pi/\omega$, the critical response always touch the negative elastic–plastic boundary $-b_0$ before upshooting beyond the level b_0. To facilitate the argument we first present a numerical study on the critical response for $n = 1$ through numerical optimization where only τ_1 and γ_1 need to be optimized because b_1 can be directly obtained from $b_1 = b_f - b_0$. A sdof system with $\omega = 2\pi\,\text{rad/s}$ (1 Hz), $\zeta = 1\%$ and $b_0 = 1$ is considered. For a given b_1, we obtain the optimal value of τ_1 by numerically optimizing the objective function

$$J(\tau_1) = A_1(\tau_1, \gamma_1, \hat{v}(\tau_1, \gamma_1, b_1), b_1)|_{\gamma_1 = t_1 - \tau_1}. \tag{35}$$

Note that the Lagrange multipliers λ_1 and λ_2 are not needed because the conditions for the final target level b_f and the failure instant t_f have already been enforced. The optimal values of γ_1 and v are obtained by $\gamma_1 = t_f - \tau_1$ and Eq. (33), respectively. The resulting f^* based on patching Eqs. (10) and (21) is optimal only when the critical response y^* is verified to obey the boundary constraints, namely $|y^*(t)| \leq b_0$ on $[0, \tau_1]$ and $\dot{y}^*(t) \geq 0$ on $[\tau_1, \tau_1 + \gamma_1]$ because these constraints have not been explicitly enforced during the optimization process.

Fig. 2 shows f^* and y^* for different values of $b_1 = 0, 1, 2, 4$ and $t_f = 0.5, 1, 2\,\text{s}$. For illustration purposes, the response y^* in this figure has been computed based on the linear-elastic Eq. (1) and the plastic Eq. (16) on $[0, \tau_1]$ and $[\tau_1, \tau_1 + \gamma_1]$, respectively. This yields the actual nonlinear response only when the boundary constraints are satisfied. The levels $+/-b_0$ that bound the elastic regime are plotted in dashed lines. The circles mark the transition points from elastic to plastic regime (first circle) and from plastic loading to the target (second circle). For $t_f = 0.5\,\text{s}$, y^* increases monotonically, passes through the yield displacement level and finally reaches the target. For $t_f = 1\,\text{s}$ or $2\,\text{s}$, y^* makes a trough before upshooting to the target. The amount of trough increases as b_1 increases. For $t_f = 2\,\text{s}$, it can be easily seen that the trough goes below the

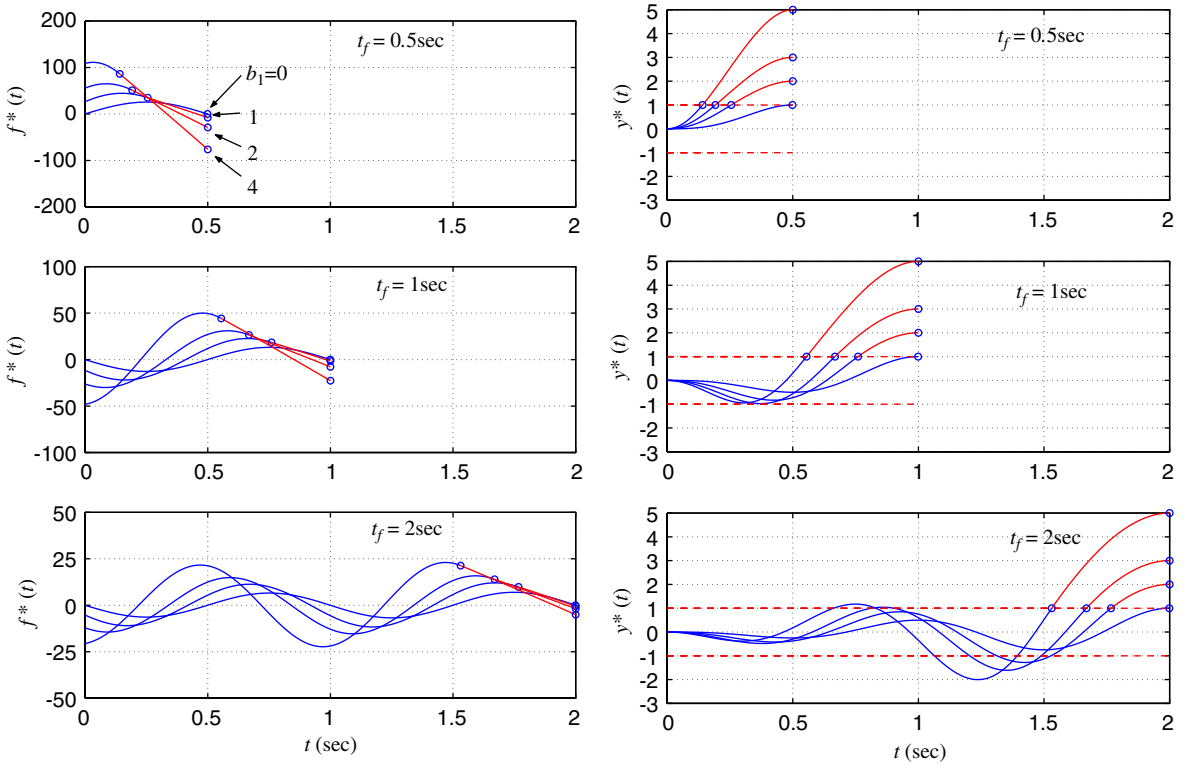

Fig. 2. Critical excitation f^* and response y^* for $n = 1$, starting from $(0, 0)$. Calculations assume system to be linear-elastic on $[0, \tau_1]$ and plastic on $[\tau_1, t_f]$.

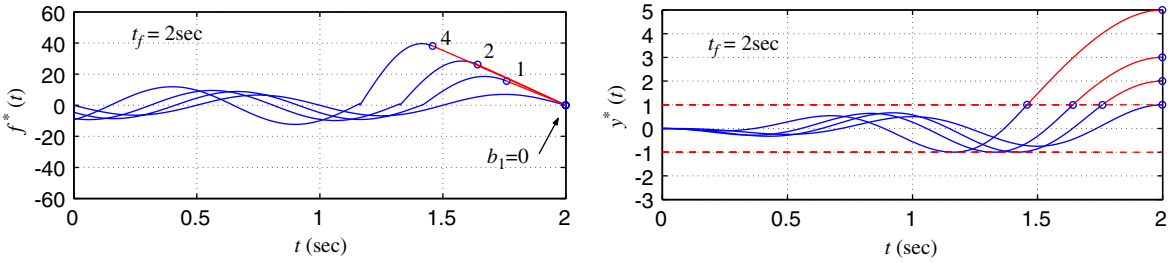

Fig. 3. Actual critical excitation f^* and response y^* for $n = 1$ (boundary constraint enforced).

negative boundary $-b_0$ for all non-zero values of b_1. In this case, f^* is no longer optimal and y^* is no longer valid because the boundary constraint is violated. Had the response been computed using time-stepping procedures following an elasto-plastic governing equation, it will undergo negative plastic deformation, and the target displacement will not be reached. This is a case where the boundary constraint is 'critical'. The actual critical response should touch the negative boundary $-b_0$ before upshooting to the target, as shown in Fig. 3. The efficient computation of the actual critical excitation in this case will be discussed later. Further numerical results show that similar observations apply to the case when the system starts from $(b_0, 0)$, which is relevant for the second and subsequent segments. Appendix D gives a further theoretical account for the occurrence of this phenomenon.

5. Boundary critical excitation

The discussion in the previous section suggests that unless the target level b_f is very close to the yield displacement b_0 or the system is required to reach a high target b_f within a very small duration t_f, the boundary constraint is active and the critical response touches the negative plastic boundary before upshooting to the target. We refer this situation as being 'boundary critical' and the corresponding critical excitation as 'boundary critical excitation'. The boundary constraints can be in principle handled by checking during numerical optimization, but this strategy is not computationally efficient. By parameterizing the critical response apriori with a boundary critical mode, the optimization problem can be further simplified.

Fig. 4 shows a candidate critical response time history, assuming it is boundary critical. The response consists of three basic blocks. The first one is the segment O–A, where the system starts from rest to the level $-b_0$ with zero velocity. The second segment is A–B–C, where the system upshoots from $-b_0$ at A to $+b_0$ at B with velocity v_1 and later produces a plastic displacement of b_1 at C. The third block is C–D, where the response enters the elastic regime again, going from the positive to the negative extreme. Subsequent phases of the response are made up by these basic blocks, by virtue of symmetry discussed in the last section. In particular, A–B–C, D–E–F and G–H–I are identical; so are C–D and F–G.

For a given n, the parameters that define the boundary critical response include t_0, t_1, s_1, t_2, v_1 and b_1. We next investigate qualitatively their optimal values, designated by a hat. First, $\hat{b}_1$ can be directly obtained from

$$\hat{b}_1 = (b_f - b_0)/n \tag{36}$$

and $\hat{v}_1$ can be obtained analytically, as discussed in Section 4.2. For the remaining parameters t_0, t_1, s_1 and t_2, note that the energy of the excitation is given by

$$E_n(t_0, t_1, s_1, t_2) = E_0(t_0) + n\,E_1(t_1, s_1) + (n-1)\,E_2(t_2), \tag{37}$$

where E_0, E_1 and E_2 are the contributions from O–A, A–B–C and C–D, respectively.

$$E_0(t_0) = \frac{1}{2}\begin{bmatrix} 0 \\ 0 \\ -b_0 \\ 0 \end{bmatrix}^{\mathrm{T}} \underline{L}_1(t_0)^{\mathrm{T}}\,\underline{H}(t_0)^{-1}\underline{L}_1(t_0) \begin{bmatrix} 0 \\ 0 \\ -b_0 \\ 0 \end{bmatrix} = \frac{b_0^2\,h_{22}(t_0)}{2\,\Delta(t_0)}, \tag{38}$$

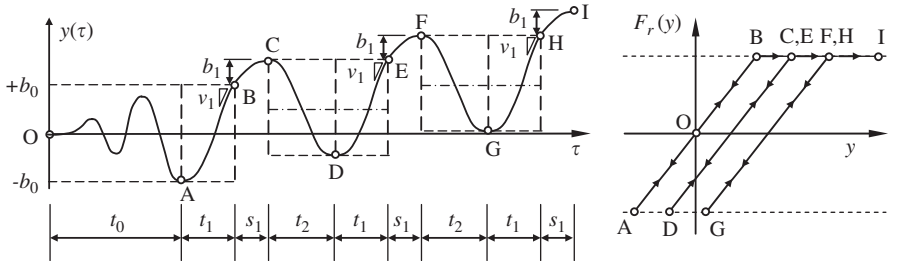

Fig. 4. Schematic diagram for boundary critical response.

$$E_1(t_1,s_1)=\frac{1}{2}\begin{bmatrix}-b_0\\0\\b_0\\\hat{v}_1\end{bmatrix}^{\mathrm{T}}\underline{L}_1(t_1)^{\mathrm{T}}\,\underline{H}(t_1)^{-1}\underline{L}_1(t_1)\begin{bmatrix}-b_0\\0\\b_0\\\hat{v}_1\end{bmatrix}+\frac{1}{2}\begin{bmatrix}b_0\\\hat{v}_1\\b_1\end{bmatrix}^{\mathrm{T}}\underline{L}_2(s_1)^{\mathrm{T}}\,\underline{R}(s_1)^{-1}\underline{L}_2(s_1)\begin{bmatrix}b_0\\\hat{v}_1\\b_1\end{bmatrix} \tag{39}$$

with $\hat{v}_1$ given by

$$\hat{v}_1(t_1,s_1)=\frac{P_{41}(t_1)-P_{43}(t_1)-Q_{21}(s_1)}{P_{44}(t_1)+Q_{22}(s_1)}b_0-\frac{Q_{23}(s_1)}{P_{44}(t_1)+Q_{22}(s_1)}b_1, \tag{40}$$

$$E_2(t_2)=\frac{1}{2}\begin{bmatrix}b_0\\0\\-b_0\\0\end{bmatrix}^{\mathrm{T}}\underline{L}_1(t_2)^{\mathrm{T}}\,\underline{H}(t_2)^{-1}\underline{L}_1(t_2)\begin{bmatrix}b_0\\0\\-b_0\\0\end{bmatrix}. \tag{41}$$

The optimal values of t_0, t_1, s_1, t_2 should minimize E_n in Eq. (37) and satisfy the failure time constraint

$$t_0+n(t_1+s_1)+(n-1)t_2=t_f. \tag{42}$$

One of the four variables can be eliminated using Eq. (42), giving a 3-D unconstrained optimization problem. Numerical experiments revealed that there exist multiple optimal solutions to this problem. These solutions essentially correspond to different locally optimal pairs of t_0 and t_2. If optimization is done numerically, it is generally difficult to ascertain whether the converged solution corresponds to the global minimum. Finding all the locally optimal solutions exhaustively generally requires a lot more computational effort than solving a convex optimization problem. An iterative procedure is next presented that can find all the local optima (and hence the global optimum) with much less computational effort by avoiding multi-dimensional search.

Consider treating the time constraint by incorporating a Lagrange multiplier λ_1 into the objective function:

$$\begin{aligned}J_n(t_0,t_1,s_1,t_2,\lambda_1)=E_0(t_0)+nE_1(t_1,s_1)+(n-1)E_2(t_2)\\+\lambda_1[t_f-t_0-n(t_1+s_1)-(n-1)\,t_2].\end{aligned} \tag{43}$$

For every λ_1, consider the set of values $\hat{t}_0(\lambda_1),\hat{t}_1(\lambda_1),\hat{s}_1(\lambda_1),\hat{t}_2(\lambda_1)$ that minimizes J_n in Eq. (43). These values do not necessarily satisfy the time constraint because the given value of λ_1 is not necessarily optimal. Instead, they correspond to some value of $\hat{t}_f=\hat{t}_0+n(\hat{t}_1+\hat{s}_1)+(n-1)\hat{t}_2$ that is generally different from the target t_f. Thus, in principle, the optimal solution can be obtained by iterating λ_1 until $\hat{t}_f$ is sufficiently close to t_f. The advantage of this approach is that the optimal values $\hat{t}_0,\hat{t}_1,\hat{s}_1,\hat{t}_2$ for each λ_1 can be obtained easily and independently of each other: $\hat{t}_0$ by minimizing $E_0(t_0)-\lambda_1 t_0$; $\hat{t}_1,\hat{s}_1$ by minimizing $E_1(t_1,s_1)-\lambda_1(t_1+s_1)$; $\hat{t}_2$ by minimizing $E_2(t_2)-\lambda_1 t_2$. This procedure is valid because the objective function in Eq. (43) is just a sum of the functions minimized. The disadvantage is that an iteration on λ_1 is required and it is difficult to know in advance the range of values where the solution of λ_1 should be sought. We next discuss further properties of λ_1 that will aid the solution process.

The optimal values of $\hat{t}_0, \hat{t}_1, \hat{s}_1, \hat{t}_2$ obtained for each value of λ_1 satisfy

$$\lambda_1 = \frac{\mathrm{d}}{\mathrm{d}t_0} E_0(\hat{t}_0) = \frac{\partial}{\partial t_1} E_1(\hat{t}_1, \hat{s}_1) = \frac{\partial}{\partial s_1} E_1(\hat{t}_1, \hat{s}_1) = \frac{\mathrm{d}}{\mathrm{d}t_2} E_2(\hat{t}_2). \tag{44}$$

Since E_0 is the energy for the system to go from $(0,0)$ to $(b_0,0)$ at time t_0, it is a positive non-increasing function of t_0. This means that $\lambda_1 = \partial E_0/\partial t_0$ is always negative. Also, the smaller the magnitude of λ_1, the larger the value of $\hat{t}_0$, and vice versa. When $\lambda_1 \to 0^-$, $t_0 \to \infty$. In the typical case of interest where t_0 is not very small, the optimal value of λ_1 will be small in magnitude.

The optimal values $\hat{t}_1$ and $\hat{s}_1$, on the other hand, are relatively insensitive to λ_1 but are strongly influenced by b_1, because they are largely dominated by resonance effects. Although decreasing the magnitude of λ_1 still has a marginal effect on increasing $\hat{t}_1$ and $\hat{s}_1$, they do not tend to infinity as $\lambda_1 \to 0^-$. Rather, they tend to nontrivial values that depend on b_1. The same is also true for the $\hat{t}_2$, but it tends to $T/2$ as $\lambda_1 \to 0^-$ regardless of b_1. This can be reasoned from the fact that when there is no time constraint, the easiest way to go from b_0 to $-b_0$ is to follow roughly the free vibration curve with initial displacement b_0 to reach $-b_0$ in a duration equal to half of the natural period.

5.1. Iterative algorithm for boundary critical excitation

Incorporating the foregoing considerations, the optimal values of t_0, t_1, s_1, t_2 for a given n can be found efficiently in an iterative manner. First, we start with $\lambda_1 = 0$ and obtain $\hat{t}_1$ and $\hat{s}_1$ by numerically minimizing (e.g., using simplex search)

$$\tilde{J}_1(t_1, s_1) = E_1(t_1, s_1) - \lambda_1(t_1 + s_1). \tag{45}$$

Given such $\hat{t}_1$ and $\hat{s}_1$, the remaining parameters t_0 and t_2 have to satisfy the time constraint $t_0 + (n-1)t_2 = t_f - n(\hat{t}_1 + \hat{s}_1)$. Using this to express t_2 in terms of t_0, and substituting into Eq. (43), the optimal value $\hat{t}_0$ for t_0 can be found by minimizing (method to be discussed shortly)

$$\tilde{J}_0(t_0) = E_0(t_0) + (n-1)E_2\left(\frac{t_f - n(\hat{t}_1 + \hat{s}_1) - t_0}{n-1}\right) \tag{46}$$

on $0 < t_0 \leq t_f - n(\hat{t}_1 + \hat{s}_1)$. The optimal value of λ_1 should be updated by

$$\lambda_1 = \frac{\partial E_0(\hat{t}_0)}{\partial t_0} = -\frac{b_0^2}{2\,\Delta(\hat{t}_0)^2}[h_{22}(\hat{t}_0)h(\hat{t}_0) - h_{12}(\hat{t}_0)\dot{h}(\hat{t}_0)]^2. \tag{47}$$

This procedure is iterated until $\hat{t}_0, \hat{t}_1, \hat{s}_1, \hat{t}_2$ have all converged. Experience shows that it normally requires only one to two iterations to achieve a relative tolerance of 1%.

The global optimal value of t_0 should be obtained by calculating the value of $\tilde{J}_0$ for a grid of values of t_0 on $[0, t_f - n(\hat{t}_1 + \hat{s}_1)]$ and then selecting the minimizing value. This procedure is able to obtain the global optimum even in the presence of multiple local optima because the whole feasible range of t_0 is exhausted by the grid values. This strategy rather than local search algorithms should be used because multiple local minima do exist. For example, Fig. 5 shows the plot of $\tilde{J}_0$ versus t_0 for an oscillator with $\omega = 2\pi$, $\zeta = 1\%$, $b_0 = 1$ targeted to reach $b_f = 2$ in time $t_f = 5$ s. The curves exhibit multiple minima, especially for intermediate values of n. Note that determining the optimal solution by selecting among a grid of values is computationally inexpensive because analytical expression for $\tilde{J}_0$ is available and only a one-dimensional grid is involved.

The algorithm presented here allows one to find the parameters that define the critical excitation for every given n. This process should be performed for $n = 1, 2, \ldots$, where the energy of the critical excitation given by Eq. (43) (note that the λ_1 term is not needed since time constraint is already satisfied) should be monitored for each n until the minimum is reached, from which the optimal value of n can be obtained.

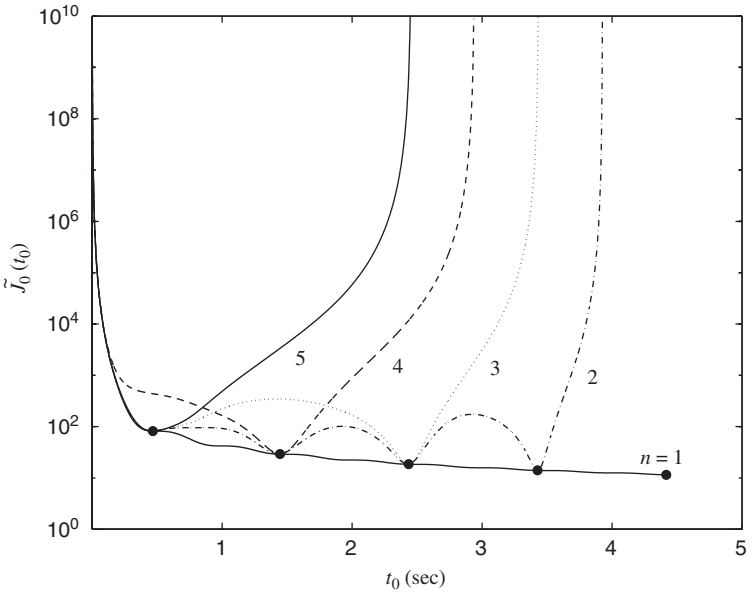

Fig. 5. Plot of $\tilde{J}_0$ versus t_0 for $t_f = 5\,\mathrm{s}$ and $b_f = 2$. Minimum points are shown by solid circles.

5.2. Checking boundary criticality

In theory, three modes of critical excitation can be distinguished, depending on whether O–A–B and/or C–D–E (and other identical blocks) are boundary critical. These modes are listed in Fig. 6. It should be noted that Mode BC3 has never been encountered in numerical experiments so far.

The criteria for checking boundary criticality are derived next. For this purpose, we introduce two new parameters, namely, $c_1 \geq 0$ and $c_2 \geq 0$ as shown in Fig. 7. Let $J_n(\underline{\theta}, \lambda_1, \lambda_2, c_1, c_2)$ be the objective function to be minimized for finding the critical excitation where the time and target constraints are incorporated through the Lagrange multipliers λ_1 and λ_2, respectively; but now it also depends on c_1 and c_2. The objective function for Mode BC1 corresponds to $J_n(\underline{\theta}, \lambda_1, \lambda_2, b_0, b_0)$. For given c_1 and c_2, let $\hat{\underline{\theta}}(c_1, c_2) = [\hat{t}_0, \hat{t}_1, \hat{s}_1, \hat{t}_2, \hat{b}_1, \hat{v}_1]^{\mathrm{T}}$, $\hat{\lambda}_1(c_1, c_2)$ and $\hat{\lambda}_2(c_1, c_2)$ be the optimal parameters that minimize $J_n(\cdot, \cdot, \cdot, c_1, c_2)$. As c_1 and c_2 changes in their 2-D space, the value of the objective function is traced by $\hat{J}_n(c_1, c_2)$:

$$\hat{J}_n(c_1, c_2) = J_n(\hat{\underline{\theta}}(c_1, c_2), \hat{\lambda}_1(c_1, c_2), \hat{\lambda}_2(c_1, c_2), c_1, c_2). \tag{48}$$

If O–A–B and C–D–E are boundary critical, then $\partial \hat{J}_n / \partial c_1 < 0$ and $\partial \hat{J}_n / \partial c_2 < 0$ at $c_1 = c_2 = b_0$. Taking partial derivatives on Eq. (48) with respect to c_i $(i = 1, 2)$,

$$\frac{\partial \hat{J}_n}{\partial c_i} = \sum_{j=1}^{6} \frac{\partial J_n}{\partial \theta_j} \frac{\partial \hat{\theta}_j}{\partial c_i} + \frac{\partial J_n}{\partial \lambda_1} \frac{\partial \hat{\lambda}_1}{\partial c_i} + \frac{\partial J_n}{\partial \lambda_2} \frac{\partial \hat{\lambda}_2}{\partial c_i} + \frac{\partial J_n}{\partial c_i}, \tag{49}$$

where $\partial J_n / \partial \theta_j$, $\partial J_n / \partial \lambda_1$, $\partial J_n / \partial \lambda_2$ are evaluated at $\underline{\theta} = \hat{\underline{\theta}}(c_1, c_2)$, $\lambda_1 = \hat{\lambda}_1(c_1, c_2)$, $\lambda_2 = \hat{\lambda}_2(c_1, c_2)$. Since by definition $\underline{\theta}$, λ_1 and λ_2 minimizes $J_n(\cdot, \cdot, \cdot, c_1, c_2)$ for given c_1 and c_2, their corresponding partial derivatives are zero. Consequently,

$$\frac{\partial \hat{J}_n}{\partial c_i} = \left. \frac{\partial J_n}{\partial c_i} \right|_{\underline{\theta} = \hat{\underline{\theta}}(c_1, c_2), \lambda_1 = \hat{\lambda}_1(c_1, c_2), \lambda_2 = \hat{\lambda}_1(c_1, c_2)}. \tag{50}$$

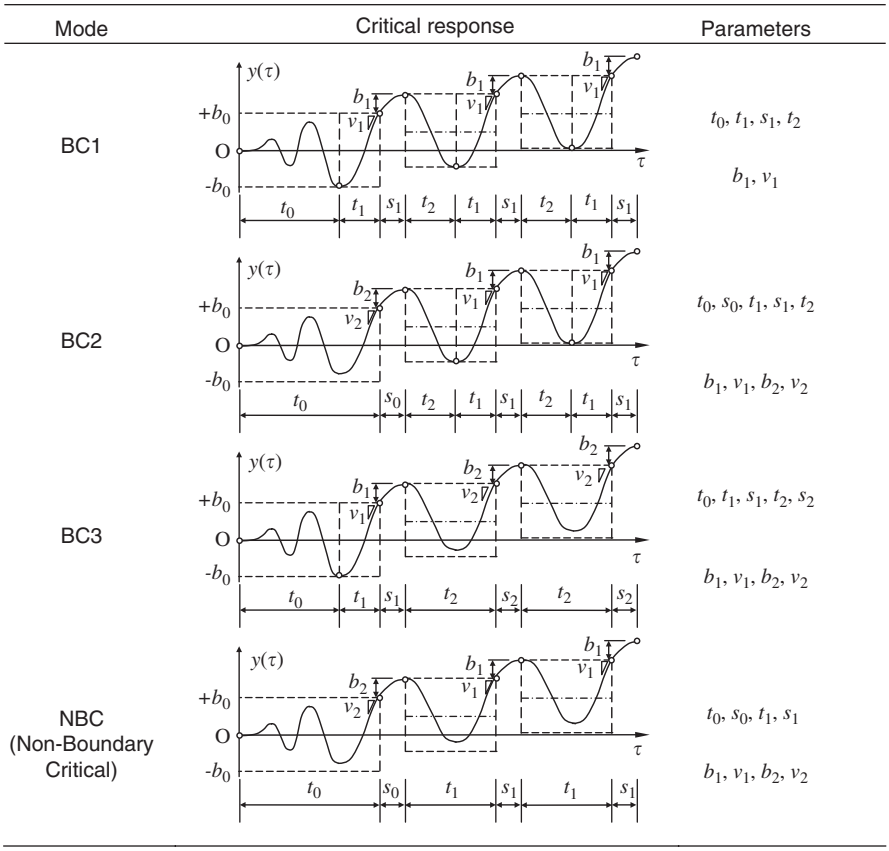

Fig. 6. Definition of boundary critical modes.

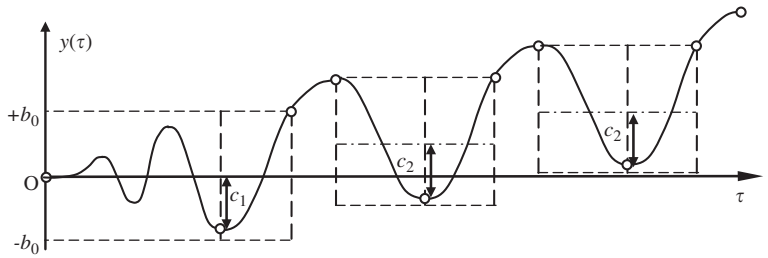

Fig. 7. Schematic diagram for non-boundary critical response.

To obtain $\partial J_n/\partial c_1$, note that

$$J_n = \frac{1}{2}\begin{bmatrix} 0 \\ 0 \\ -c_1 \\ 0 \end{bmatrix}^{\mathrm{T}} \underline{L}_1(t_0)^{\mathrm{T}}\, \underline{H}(t_0)^{-1}\, \underline{L}_1(t_0) \begin{bmatrix} 0 \\ 0 \\ -c_1 \\ 0 \end{bmatrix} + \frac{1}{2}\begin{bmatrix} -c_1 \\ 0 \\ b_0 \\ v_1 \end{bmatrix}^{\mathrm{T}} \underline{L}_1(t_1)^{\mathrm{T}}\, \underline{H}(t_1)^{-1}\, \underline{L}_1(t_1) \begin{bmatrix} -c_1 \\ 0 \\ b_0 \\ v_1 \end{bmatrix}$$
$$+ \text{other terms independent of } c_1 \tag{51}$$

and so is a quadratic function of c_1. Its derivative can be easily obtained as

$$\frac{\partial J_n}{\partial c_1} = [P_{33}(t_0) + P_{11}(t_1)]\, c_1 - P_{13}(t_1) b_0 - P_{14}(t_1) v_1, \tag{52}$$

where P_{ij} can be obtained from Appendix B. Thus, let t_0^*, t_1^*, v_1^* be the values obtained from the iterative algorithm assuming Mode BC1, O–A–B is boundary critical if

$$P_{14}(t_1^*) v_1^* > [P_{33}(t_0^*) + P_{11}(t_1^*) - P_{13}(t_1^*)] b_0. \tag{53}$$

For C–D–E, by noting that

$$J_n = \frac{n-1}{2} \begin{bmatrix} b_0 \\ 0 \\ -c_2 \\ 0 \end{bmatrix}^{\mathrm{T}} \underline{L}_1(t_2)^{\mathrm{T}}\, \underline{H}(t_2)^{-1}\, \underline{L}_1(t_2) \begin{bmatrix} b_0 \\ 0 \\ -c_2 \\ 0 \end{bmatrix} + \frac{n-1}{2} \begin{bmatrix} -c_2 \\ 0 \\ b_0 \\ v_2 \end{bmatrix}^{\mathrm{T}} \underline{L}_1(t_1)^{\mathrm{T}}\, \underline{H}(t_1)^{-1}\, \underline{L}_1(t_1) \begin{bmatrix} -c_2 \\ 0 \\ b_0 \\ v_2 \end{bmatrix}$$
$$+ \text{other terms independent of } c_2 \tag{54}$$

and following a similar procedure, it can be shown that C–D–E is boundary critical if

$$P_{14}(t_1^*) v_1^* > [P_{33}(t_2^*) + P_{11}(t_1^*) - P_{13}(t_1^*) - P_{13}(t_2^*)] b_0. \tag{55}$$

The formulas for checking boundary criticality are based on the optimal values of the parameters and so they provide only sufficient conditions. For example, if $\partial J_n/\partial c_1 < 0$ and $\partial J_n/\partial c_2 < 0$, then the boundary critical solution is valid. Otherwise, if $\partial J_n/\partial c_1 > 0$ but $\partial J_n/\partial c_2 < 0$, it only suggests that O–A–B is not boundary critical but C–D–E is. In this case the boundary criticality assumption of O–A–B should be relaxed and a new solution is obtained assuming Mode BC2. The solution in this case can be efficiently obtained by further iterations. After that, boundary criticality of C–D–E should be checked again, since the optimal parameters have changed.

6. Numerical study

Using the proposed method, we determined the critical excitations for an elasto-plastic oscillator with $\omega = 2\pi$ (1 Hz), $\zeta = 1\%$ and $b_0 = 1$. The results are shown in Fig. 8 for the first passage time $t_f = 5$ s and different values of target threshold $b_f = 2, 3, 4$. All cases are found to be boundary critical (BC1). The transition points between different segments are marked with a heavy dot. For discussion purposes, the transition points for Case (b) (second row) have been named with alphabets, which correspond to the same points in Fig. 4. The segments B–C, E–F and H–I are in the plastic regime, while the rest are in the linear-elastic regime.

The initial phase (O–A) of the critical excitation is just the unit impulse response going in reverse time. During A–B where the response is prepared to upshoot beyond the yield level b_0, the critical excitation has a larger amplitude than that before first yielding. Within B–C where the response is increasing in the plastic regime, the excitation appears to complete the sinusoidal trend, although in fact it follows an exponential trend (see Eq. (21)). From C to D where the system returns to the elastic regime again through unloading, the excitation takes on small values. This is intuitive because during this phase the response can drop primarily by its own elastic restoring force to its minimum even in the absence of external force. The excitation in this case only provides the necessary force to compensate for the energy loss due to damping as the system goes from C to D; otherwise, by damped free vibration the response can only reach down to some level slightly above $-b_0$.

The critical excitation resonates with the system in the elastic regime (A–B) where the system gains momentum to shoot through the yield level b_0. Little energy is spent when the response drops from C to D, as it can be accomplished primarily by free vibration. The 'tapering' of the excitation during C–D is an important feature that generates a large response efficiently. If the excitation continues to have the same amplitude as the previous cycle, it will drive the response to have negative plastic deformation that cancels out the previous plastic response. This feature of critical excitation is unique to hysteretic systems and is not observed in linear systems. The resulting hysteretic curve exhibits a 'drift' type of oscillation [16].

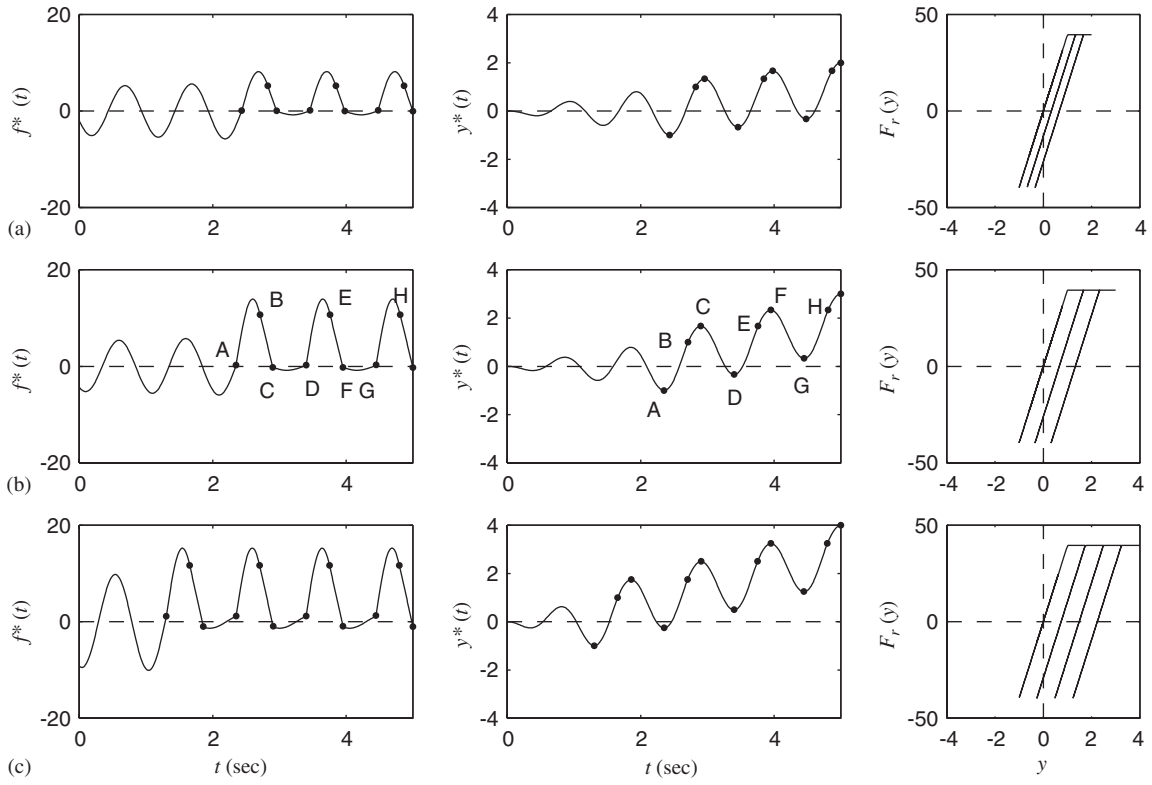

Fig. 8. Critical excitation f^*, critical response y^* and restoring force F_r for $t_f = 5$ s and different values of b_f. (a) $b_f = 2$; (b) $b_f = 3$; (c) $b_f = 4$. Transition points between different segments are marked by heavy dots.

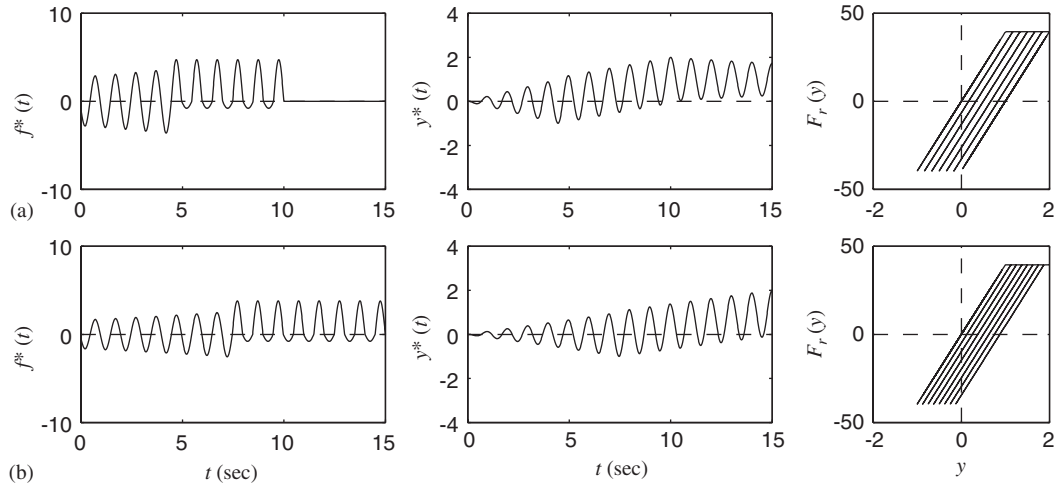

Fig. 9. Critical excitation f^*, critical response y^* and restoring force F_r for $b_f = 2$ and different values of t_f. (a) $t_f = 5$ s; (b) $t_f = 10$ s; (c) $t_f = 15$ s. Transition points between different segments are marked by heavy dots.

Fig. 9 shows the critical excitations for $t_f = 10$ and 15 s. It is seen that when the oscillator is given more time to reach its target, the critical excitation spends more hysteretic cycles to reach its target. Meanwhile, the duration before first yielding also increases. The results are qualitatively the same as those in Fig. 8.

Fig. 10 shows the energy of the critical excitation for different values of n. Note that the critical excitations shown in Figs. 8 and 9 correspond to the optimal value of n (marked with a solid circle) that minimizes the

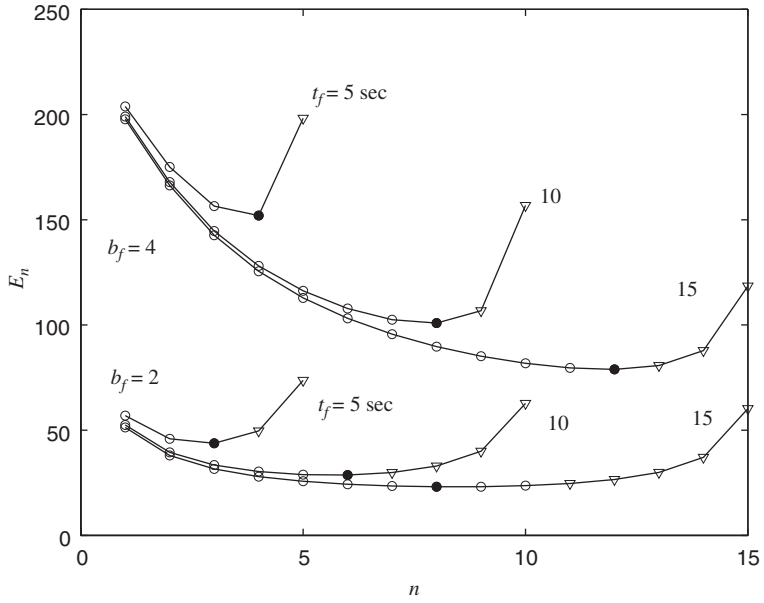

Fig. 10. Plot of energy versus n for critical excitations. Minimum points are shown by solid circles; non-boundary critical cases are shown by inverted triangles.

energy. The lower and upper set of curves correspond to $b_f = 2$ and $b_f = 4$, respectively. The energy curve always decrease initially when n increases from 1. This is when the initial elastic phase is given the majority of time span to develop but each subsequent plastic phase has to generate a relatively large plastic displacement b_1 so as to reach the target b_f, because n is small.

The inverted triangles in Fig. 10 denote the non-boundary critical cases, where the actual solution is obtained by further iterations. The non-boundary critical cases all correspond to BC2 (see Fig. 7), as a result of the fact that n is too large, i.e., too many oscillations, that leaves little time for each oscillation to gain momentum in the elastic regime, resulting in a sub-optimal configuration. This is also the reason for the dramatic increase in energy when n is too large, say, when n is approximately equal to the number of natural periods within t_f, i.e., $n \approx t_f/(2\pi/\omega)$. Nevertheless, the non-boundary critical cases are of little practical significance because they occur after the minimum point is reached and when n is large. If the whole energy curve is not needed and only the final optimal n is required, one can start with some initial guess for n and then search locally to reach the optimum. In this case at most one non-boundary critical case will be encountered.

7. Concluding remarks

This study shows that, although resonance is still a primary characteristics of critical excitations for elasto-plastic systems, a new mechanism called 'boundary criticality' accounts for the drift behavior in the critical response where opposing plastic deformation is avoided. It is not present for linear systems because in that case no hysteresis is involved.

In contrast to stable linear systems where infinitesimal perturbations in the excitation leads to infinitesimal perturbations in the response, the response of elasto-plastic systems can be quite sensitive to small infinitesimal perturbations in the excitation. The latter may cause plastic deformation that can accumulate and change the subsequent regime (elastic or plastic) through which the response will take place, resulting in perturbations in the response that is no longer infinitesimal. This has implications in, for example, whether the knowledge of critical excitations can help construct an efficient importance sampling density for estimating the first passage probabilities of elasto-plastic systems by importance sampling method [24]. In the linear case, the knowledge about critical excitations can lead to very efficient estimation of first passage probabilities [4]. Applying the findings in this study to stochastic analysis of elasto-plastic systems will be a future topic of research.

The case of mdof system is obviously more complicated that the sdof case. One complication arises from the fact that different elasto-plastic elements of the mdof system may undergo different phases of motion (elastic loading/unloading, plastic loading), requiring a far more complicated parameterization scheme in the time domain (if ever attempted). Nevertheless, the basic characteristics of the critical excitation in the sdof case may well apply to the mdof case, and this will help constructing approximate (suboptimal) critical excitations for mdof systems that may suffice in many applications. This will be a further topic of research.

Acknowledgment

This paper is based upon work supported by University Grant 7200053, City University of Hong Kong. The support is gratefully acknowledged.

Appendix A. Critical response has no opposing plastic deformation

This appendix shows that the critical response cannot have opposing plastic deformation. In particular, we show that for any segment of response that has an opposing plastic deformation, one can always construct a counterpart that has the same boundary states but it has no opposing plastic deformation and its associated excitation has less energy. Two cases need to be considered, namely, one that starts from zero initial conditions and the other one starting from b_0 with zero initial velocity. The first case will be considered first; the second one follows in a similar manner.

Fig. 11 shows the schematic diagrams for the two cases. In both cases, y is the response that has a negative plastic deformation Δ at some time instant τ_1 before reaching the final displacement level b_0+b_1 with zero velocity at τ_2. Let $E_1(b,t)$ and $E_2(b,t)$ denote respectively the smallest energy required to drive the elasto-plastic system to the displacement level b with zero velocity at time t, from the initial conditions $(0,0)$ and $(-b_0,0)$. It is clear that, for a given t, $E_1(b,t)$ is a non-decreasing function of b and so is $E_2(b,t)$ for $b>b_0$.

Let $E(y)$ be the energy of the excitation corresponding to y in Case 1 (Fig. 11(a)). For any $\Delta>0$,

$$E(y) \geq E_1(b_0+\Delta,\tau_1)+E_2(b_0+b_1+\Delta,\tau_2-\tau_1). \tag{56}$$

Now consider the critical response y_c that is to touch the level $-b_0$ at τ_1 and then upshoot to the level b_0+b_1 at τ_2. Then

$$\begin{aligned} E(y_c) &= E_1(b_0,\tau_1)+E_2(b_0+b_1,\tau_2-\tau_1) \\ &\leq E_1(b_0+\Delta,\tau_1)+E_2(b_0+b_1+\Delta,\tau_2-\tau_1) \leq E(y) \end{aligned} \tag{57}$$

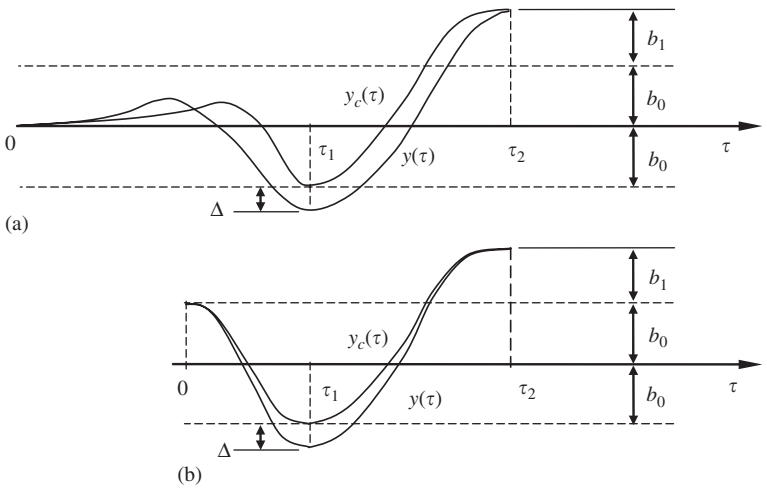

Fig. 11. Schematic diagram for Appendix A.

and so y is always sub-optimal to y_c, i.e., the energy can always be reduced by eliminating negative plastic deformation.

A similar argument can be applied for Case 2. In this case, for y and y_c in Fig. 11(b),

$$\begin{aligned} E(y) &\geq E_2(b_0+\Delta,\tau_1)+E_2(b_0+b_1+\Delta,\tau_2-\tau_1) \\ &\geq E_2(b_0,\tau_1)+E_2(b_0+b_1,\tau_2-\tau_1)=E(y_c). \end{aligned} \tag{58}$$

Appendix B. Expressions for P and Q

For $P(t)=\underline{L}_1(t)^T\,\underline{H}(t)^{-1}\underline{L}_1(t)$, its entries are given by (dependence on t is omitted for brevity)

$$P_{11}=(g^2h_{22}-2g\dot{g}h_{12}+\dot{g}^2h_{11})/\Delta_1,\quad P_{12}=(hgh_{22}-h\dot{g}h_{12}-\dot{h}g\,h_{12}+\dot{h}\dot{g}h_{11})/\Delta_1,$$

$$P_{13}=(-gh_{22}+\dot{g}h_{12})/\Delta_1,\quad P_{14}=(gh_{12}-\dot{g}h_{11})/\Delta_1,\quad P_{22}=(h^2h_{22}-2h\,\dot{h}\,h_{12}+\dot{h}^2h_{11})/\Delta_1,$$

$$P_{23}=(-h\,h_{22}+\dot{h}h_{12})/\Delta_1,\quad P_{24}=(h\,h_{12}-\dot{h}h_{11})/\Delta_1,$$

$$P_{33}=h_{22}/\Delta_1,\quad P_{34}=-h_{12}/\Delta_1,\quad P_{44}=h_{11}/\Delta_1, \tag{59}$$

where $\Delta_1=|\underline{H}|=h_{11}h_{22}-h_{12}^2$.

For $Q(t)=\underline{L}_2(t)^T\,\underline{R}(t)^{-1}\underline{L}_2(t)$, its entries are given by

$$Q_{11}=\omega^4(r_1^2r_{22}-2r_1r\,r_{12}+r^2r_{11})/\Delta_2,\quad Q_{12}=\omega^2(-r\,r_1r_{22}+r^2r_{12}+\dot{r}\,r_1r_{12}-\dot{r}r\,r_{11})/\Delta_2,$$

$$Q_{13}=-\omega^2(-r_1r_{22}+r\,r_{12})/\Delta_2,\quad Q_{22}=(r^2r_{22}-2r\,\dot{r}\,r_{12}+\dot{r}^2r_{11})/\Delta_2,$$

$$Q_{23}=-(r\,r_{22}-\dot{r}r_{12})/\Delta_2,\quad Q_{33}=r_{22}/\Delta_2, \tag{60}$$

where $\Delta_2=|\underline{R}|=r_{11}r_{22}-r_{12}^2$ and $r_1=\int_0^t r\,\mathrm{d}\tau$.

Appendix C. Interpretation of optimality condition

In this appendix, we show that the optimality condition $\partial A_1/\partial v_1=0$ in Eq. (32) is equivalent to requiring that the excitation be continuous at the transition point (Eq. (64)).

Let $\underline{\beta}$ and $\underline{\chi}$ be the vectors of Lagrange multipliers for the consecutive time segments spanned by τ_1 (linear-elastic phase) and γ_1 (plastic loading phase), respectively. Then

$$\underline{\beta}=\underline{H}(\tau_1)^{-1}\,\underline{L}_1(\tau_1)\begin{bmatrix}0\\0\\b_0\\v_1\end{bmatrix},\quad \begin{bmatrix}0\\0\\0\\1\end{bmatrix}^{\mathrm{T}}\underline{L}_1(\tau_1)^{\mathrm{T}}=[0\quad 1] \tag{61}$$

and

$$\underline{\chi}=\underline{R}^{-1}(\gamma_1)\,\underline{L}_2(\gamma_1)\begin{bmatrix}b_0\\v_1\\b_1\end{bmatrix},\quad \begin{bmatrix}0\\1\\0\end{bmatrix}^{\mathrm{T}}\underline{L}_2(\gamma_1)^{\mathrm{T}}=-[r(\gamma_1)\quad \dot{r}(\gamma_1)]. \tag{62}$$

Eq. (32) can thus be written as

$$\frac{\partial A_1}{\partial v_1}=[0\quad 1]\,\underline{\beta}-[r(\gamma_1)\quad \dot{r}(\gamma_1)]\,\underline{\chi}. \tag{63}$$

On the other hand, the critical excitation on the interval spanned by τ_1 is $f_1^*(\tau)=[h(\tau_1-\tau),\dot{h}(\tau_1-\tau)]\,\underline{\beta}$, and so $f_1^*(\tau_1)=[0,1]\,\underline{\beta}$, since $h(0)=1$ and $\dot{h}(0)=1$. Taking the instant τ_1 as the origin, the critical excitation on the interval spanned by γ_1 is $f_2^*(\tau)=[r(\gamma_1-\tau),\dot{r}(\gamma_1-\tau)]\,\underline{\chi}$, and so $f_2^*(0)=[r(\gamma_1),\dot{r}(\gamma_1)]\,\underline{\chi}$. Substituting these

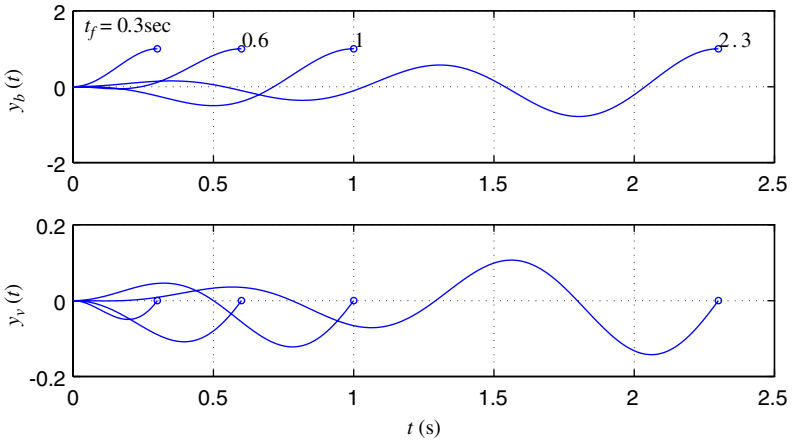

Fig. 12. Critical response y_b and y_v.

relations into Eq. (63) and setting it to zero gives

$$f_1^*(\tau_1) = f_2^*(0) \tag{64}$$

which means that optimality in v_1 requires the critical excitation be continuous at the transition point between the elastic and plastic regime.

Appendix D. Further discussions on boundary criticality

In this appendix, we give a theoretical account for the occurrence of boundary criticality described in Section 4.3. Consider the critical excitation in the linear-elastic regime that starts from $(0,0)$ to (b_0, v). The critical excitation is given by $f = \beta_1 h(t-\tau) + \beta_2 \dot{h}(t-\tau)$ where

$$\underline{\beta} = \begin{bmatrix} h_{11} & h_{12} \\ h_{12} & h_{22} \end{bmatrix}^{-1} \begin{bmatrix} b_0 \\ v \end{bmatrix} = \frac{1}{\Delta} \begin{bmatrix} h_{22} & -h_{12} \\ -h_{12} & h_{22} \end{bmatrix} \begin{bmatrix} b_0 \\ v \end{bmatrix} = \underline{\beta}_b b_0 + \underline{\beta}_v v \tag{65}$$

and $\Delta = |\underline{H}| = h_{11}h_{22} - h_{12}^2$, $\underline{\beta}_b = [h_{22}, -h_{12}]^{\mathrm{T}}/\Delta$ and $\underline{\beta}_v = [-h_{12}, -h_{11}]^{\mathrm{T}}/\Delta$. The critical response y_b (say) corresponding to $\underline{\beta}_b$ goes from $(0,0)$ to $(1,0)$ on the $(y, \dot{y})$ state-space. On the other hand, the critical response y_v (say) corresponding to $\underline{\beta}_v$ goes from $(0,0)$ to $(0,1)$. Fig. 12 shows the time history of y_b and y_v for different values of t_f. It can be seen that y_b increases in an oscillatory manner to its target without overshooting before t_f, i.e., $|y_b(t)| < 1$ for all $t < t_f$. On the other hand, y_v can have quite large displacements before t_f because only its final velocity is constrained. Roughly speaking, y_b and y_v are out of phase, i.e., y_b achieves its maximum or minimum value at approximately the same instant when y_v is around zero, and vice versa.

The response corresponding to the critical excitation that drives the system from $(0,0)$ to (b_0, v) is given by

$$y(t) = b_0\, y_b(t) + v y_v(t). \tag{66}$$

It is important to note from Fig. 12 that, shortly before y_v achieves its target velocity at t_f, it is always negative. This is the essential cause for why the critical response in Fig. 2 tends to overshoot into the negative plastic regime before upshooting to (b_0, v). In particular, let $\hat{\tau}$ be the time at which y_v achieves its last trough. Then, since y_b is approximately out of phase with y_v, $y(\hat{\tau}) = b_0\, y_b(\hat{\tau}) + v y_v(\hat{\tau}) \approx v y_v(\hat{\tau})$ as $y_b(\hat{\tau}) \approx 0$. Thus, for sufficiently large v, it can happen that $y(\hat{\tau}) < -b_0$, violating the linear-elastic regime constraint.

References

[1] A. Papoulis, Maximum response with input energy constraints and the matched filter principle, *IEEE Transactions of Circuit Theory* 17 (2) (1970) 175–182.
[2] R.F. Drenick, Model-free design of aseismic structures, *Journal of Engineering Mechanics, ASCE* 96 (1970) 483–493.
[3] K. Zhou, J. Doyle, K. Glover, *Robust and Optimal Control*, Prentice-Hall, Englewood Cliffs, NJ, 1996.

[4] S.K. Au, J.L. Beck, First-excursion probabilities for linear systems by very efficient importance sampling, *Probabilistic Engineering Mechanics* 16 (3) (2001) 193–207.
[5] A. Der Kiureghian, The geometry of random vibrations and solutions by FORM and SORM, *Probabilistic Engineering Mechanics* 15 (1) (2000) 81–90.
[6] G.Q. Cai, Y.K. Lin, Reliability of nonlinear structural frame under seismic excitation, *Journal of Engineering Mechanics, ASCE* 124 (8) (1998) 852–856.
[7] A.K. Chopra, C. Chintanapakdee, Comparing response of SDF systems to near-fault and far-fault earthquake motions in the context of spectral regions, *Earthquake Engineering and Structural Dynamics* 30 (2001) 1769–1789.
[8] N.J. Tarp-Johansen, O. Ditlevsen, Time between plastic displacements of elasto-plastic oscillators subjected gaussian white noise, *Probabilistic Engineering Mechanics* 16 (2001) 373–380.
[9] D. Vian, M. Bruneau, Tests to structural collapse of single degree of freedom frames subjected to earthquake excitations, *Journal of Engineering Mechanics, ASCE* 129 (12) (2003) 1676–1685.
[10] J.W. Lindt, G. Goh, Effect of earthquake duration on structural reliability, *Engineering Structures* 26 (2004) 1585–1597.
[11] J. Hancock, J.J. Bommer, The effective number of cycles of earthquake ground motion, *Earthquake Engineering and Structural Dynamics* 34 (2005) 637–664.
[12] R. Iyengar, C.S. Manohar, Nonstationary random critical seismic excitations, *Journal of Engineering Mechanics, ASCE* 113 (4) (1987) 529–541.
[13] R. Srinivasan, R. Corotis, B. Ellingwood, Generation of critical stochastic earthquakes, *Earthquake Engineering and Structural Dynamics* 21 (1992) 275–288.
[14] I. Takewaki, A new method for nonstationary random critical excitation, *Earthquake Engineering and Structural Dynamics* 30 (4) (2001) 519–535.
[15] R.N. Iyengar, Worst inputs and a bound on the highest peak statistics of a class of non-linear systems, *Journal of Sound and Vibration* 25 (1) (1972) 29–37.
[16] B.D. Westermo, The critical excitation and response of simple dynamic systems, *Journal of Sound and Vibration* 100 (2) (1985) 233–242.
[17] T.K. Caughey, Random excitation of a system with bilinear hysteresis, *Journal of Applied Mechanics* (1960) 649–652.
[18] J.B. Roberts, P.D. Spanos, *Random Vibration and Statistical Linearization*, Wiley, New York, USA, 1990.
[19] R.F. Drenick, The critical excitation of nonlienar systems, *Journal of Applied Mechanics* (1977) 333–336.
[20] A.J. Philippacopoulos, P.C. Wang, Seismic inputs for nonlinear structures, *Journal of Engineering Mechanics, ASCE* 110 (1984) 828–836.
[21] I. Takewaki, Critical excitation for elastic–plastic structures via statistical equivalent linearization, *Probabilistic Engineering Mechanics* 17 (1) (2002) 73–84.
[22] H. Koo, A. Der Kiureghian, K. Fujimura, Design-point excitation for non-linear random vibrations, *Probabilistic Engineering Mechanics* 20 (2) (2005) 136–147.
[23] S.K. Au, On the Solution of First Excursion Problems by Simulation with Applications to Probabilistic Seismic Performance Assessment, PhD Thesis in Civil Engineering, EERL Report No. 2001-02, California Institute of Technology, Pasadena, 2001.
[24] J.M. Hammersley, D.C. Handscomb, *Monte-Carlo Methods*, Methuen, London, 1964.